

**Figure 30.** Poiseuille flow for low, medium, and high Reynolds number.

## 5 Instabilities

We started these lectures by studying some simple, laminar flows in which the fluid moves smoothly through space. One important question that we haven't yet addressed is: are these flows stable? If we perturb them in some way, does the flow persist or does it get driven to something more complicated?

The answer is that many flows, even very simple ones, can be unstable. This statement is especially true at high Reynolds number, where viscosity fails to dampen the perturbations. You can see an example in the photographs<sup>9</sup> of Poiseuille flow, describing fluid flowing down a pipe, shown in Figure 30. The fluid in the pictures is transparent and the flow is moving from left to right, but some black dye is released from the same point on the left-hand edge and traces out what is known as a *streakline*. (For time independent flows, it coincides with both the path line and the streamline that we introduced previously. For time dependent flows, it differs.)

The top picture shows the flow when it is slow, so that  $Re \lesssim 1$  and the fluid is well described by the solution that we already met in Section 3.2.3. The flow is laminar, with the velocity field lying parallel to the pipe and the picture looks boring:

But as the flow speeds up, so that  $Re \sim 100$  or so, things become more interesting. This is shown in the middle picture where the streakline starts to wobble in places,

---

<sup>9</sup>These pictures are snapshots from this [Youtube video](#). You can also find remarkably similar pictures drawn by Reynolds in his [original paper from 1883](#).

with the wobbles dragged along by the flow. This is the manifestation of instabilities of the simple solution.

Finally, by the time we are in the regime  $Re \sim 10^3$  or  $10^4$  (the exact number depends on how rough the boundary of the pipe is), the flow appears qualitatively different yet again. This is shown in the bottom figure. Any clearly defined wobbles have vanished. The flow just looks messy. This is the turbulent regime.

Our goal in this section is to start to understand these kinds of instabilities. Although Poiseuille and Couette are the simplest examples of laminar flows, it turns out that understanding their instabilities is not so straightforward. For this reason, we start by looking at specific instabilities in other contexts. (For what it's worth, our instabilities of choice are the Kelvin-Helmholtz instability, the Plateau-Rayleigh instability, and the Rayleigh-Bénard instability. We'll see what these names mean as we proceed.)

Our method to analyse instabilities will mirror the analysis of waves in Section 4. That is: we start with some background flow and perturb it. The perturbations that we call waves oscillate back and forth about the original flow. In contrast, the unstable perturbations that we will meet here grow without bound. These are known as *linear instabilities*. Our linear analysis only shows the beginning of the instability, rather than the end point of the flow, but with some imaginative thinking (and the help of experiment!) we can figure out the qualitative form of the final flow.

With these successes in hand, we then turn to understand the stability of seemingly simpler flows, like Couette flow and Poiseuille flow that we met in Section 3.2. As we mentioned above, it turns out that understanding the fate of these flows is somewhat harder. We will succeed in giving some general results about when flows of this kind are stable against linear perturbations and when they are not. However, as we explain, these results do not stand up particularly well against either experiment or numerical simulation. This is because, ultimately, these flows have more complicated *non-linear instabilities* where an arbitrarily small perturbation is innocuous, but the instability manifests itself only when the perturbation grows to a certain size. We will not study these non-linear instabilities in these lectures.

There are a number of other topics that we won't touch upon. These include transitory phenomenon, and the transition to turbulence, with features characteristic of chaos such as period doubling and the appearance of strange attractors. We will however describe some aspects of fully developed turbulence in Section 6.

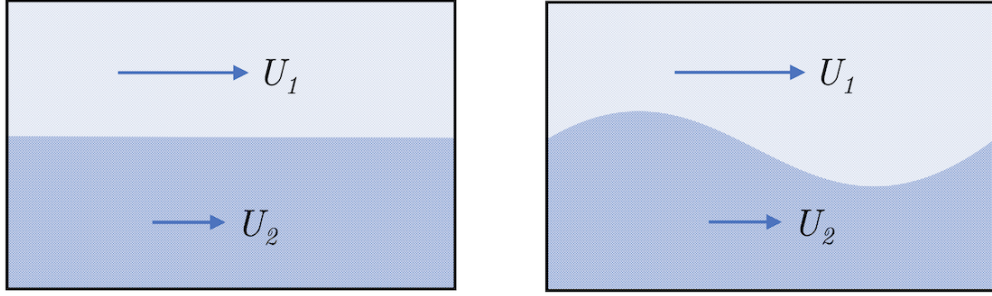


**Figure 31.** The Kelvin-Helmholtz instability between two moving fluids. The left-hand figure is unstable to turn into the right.

### 5.1 Kelvin-Helmholtz Instability

The set-up is straightforward. We have two fluids, with densities  $\rho_1 \leq \rho_2$ . The lighter fluid sits on top and travels with constant speed  $U_1$  in the  $x$ -direction. The heavier fluid sits at the bottom and travels with constant speed  $U_2 \neq U_1$  in the same direction. Initially, there is an interface between the two at  $z = 0$  as shown in Figure 31.

The initial velocity profile has a discontinuity at  $z = 0$ . In reality, this will be smoothed out by a thin layer in which viscosity is important. For our purposes, we'll neglect this and study the flow using the Euler equation for each fluid,

$$\rho_i \left( \frac{\partial \mathbf{u}_i}{\partial t} + \mathbf{u}_i \cdot \nabla \mathbf{u}_i \right) = -\nabla P_i + \rho_i \mathbf{g} \quad i = 1, 2$$

Note that we've included the effect of gravity on the right-hand side. It turns out that this won't be necessary to exhibit the physics that we're interested in, but it does have an interesting role to play.

We want to understand whether the initial flow is stable. (Spoiler: it won't be!) In particular, we'll look at perturbations in which the interface is perturbed to

$$z = \eta(x, t) = \eta_0 e^{ikx - i\omega t} \quad (5.1)$$

In other words, we're looking for an instability in which the interface develops waves.

The analysis is almost identical to that of Section 4.1 where we first met surface waves. We look for 2d flows, with  $\mathbf{u} = \mathbf{u}(x, z, t)$ . We will assume that the flow remains irrotational after the perturbation, so we introduce velocity potentials and write

$$\mathbf{u} = \begin{cases} \mathbf{U}_1 + \nabla \phi_1 & z > \eta \\ \mathbf{U}_2 + \nabla \phi_2 & z < \eta \end{cases}$$

where  $\mathbf{U}_i = U_i \hat{\mathbf{x}}$ . The requirement that the fluid is incompressible then means that we must, once again, solve the Laplace equation

$$\nabla^2 \phi_1 = \nabla^2 \phi_2 = 0$$

As usual, all the subtleties lie in the boundary conditions. We require that the fluid returns to its initial state asymptotically, so  $\phi_1 \rightarrow 0$  as  $z \rightarrow \infty$  and  $\phi_2 \rightarrow 0$  as  $z \rightarrow -\infty$ . On the interface, we impose the free boundary condition that we described previously in (4.6)

$$u_z = \frac{D\eta}{Dt}$$

This now reads

$$\left. \frac{\partial \phi_i}{\partial z} \right|_{z=\eta} = \frac{\partial \eta}{\partial t} + \left( U_i + \left. \frac{\partial \phi_i}{\partial x} \right|_{z=\eta} \right) \frac{\partial \eta}{\partial x} \quad i = 1, 2 \quad (5.2)$$

Finally, the pressure forces on either side of the interface must balance the surface tension,

$$P_2(x, \eta) - P_1(x, \eta) = -\gamma \frac{\partial^2 \eta}{\partial x^2} \quad (5.3)$$

with  $\gamma$  the surface tension. Rather like gravity, it will turn out that the presence of surface tension is unnecessary to explain the main physics point that we're interested in, but has an interesting implication later on.

To implement the pressure difference equation, we follow the analysis of Section 4.1.2 and use the Bernoulli principle. The analog of our earlier result (4.7) is now

$$\rho_i \frac{\partial \phi_i}{\partial t} + \frac{1}{2} \rho_i |\mathbf{U}_i + \nabla \phi_i|^2 + P_i + \rho_i g z = f_i(t) \quad i = 1, 2$$

with  $f_i(t)$  independent of space. The condition (5.3) then becomes

$$\begin{aligned} \rho_1 \left( \left. \frac{\partial \phi_1}{\partial t} + \frac{1}{2} |\mathbf{U}_1 + \nabla \phi_1|^2 + g z \right|_{z=\eta} \right) \\ - \rho_2 \left( \left. \frac{\partial \phi_2}{\partial t} + \frac{1}{2} |\mathbf{U}_2 + \nabla \phi_2|^2 + g z \right|_{z=\eta} \right) = \tilde{f}(t) - \gamma \frac{\partial^2 \eta}{\partial x^2} \end{aligned} \quad (5.4)$$

for some spatially-independent function  $\tilde{f}(t)$ . This, then, is our goal. Solve the Laplace equations subject to (5.2) and (5.4).

## The Linearised Approximation

As for surface waves, we make progress by assuming that the amplitude of the perturbation is small. For us, this means

$$k\eta_0 \ll 1$$

This allows us to linearise the boundary conditions (5.2) and (5.4). The first (5.2) becomes

$$\left. \frac{\partial \phi_i}{\partial z} \right|_{z=0} = \frac{\partial \eta}{\partial t} + U_i \left. \frac{\partial \eta}{\partial x} \right|_{z=0} \quad i = 1, 2 \quad (5.5)$$

while (5.4) becomes

$$\rho_1 \left( \frac{\partial \phi_1}{\partial t} + U_1 \frac{\partial \phi_1}{\partial x} \right)_{z=0} - \rho_2 \left( \frac{\partial \phi_2}{\partial t} + U_2 \frac{\partial \phi_2}{\partial x} \right)_{z=0} + g(\rho_1 - \rho_2)\eta = \tilde{f}(t) - \gamma \frac{\partial^2 \eta}{\partial x^2} \quad (5.6)$$

Now we have something eminently more achievable on our hands: solve the Laplace equations subject to (5.5) and (5.6).

### 5.1.1 The Simplest Instability

To illustrate the key idea, we first ignore both gravity and surface tension. This means that we set  $g = \gamma = 0$  in (5.6). We've already shown our hand for the kind of perturbation (5.1) of the interface that we're looking for. We augment this with a commensurate wavy solution for the velocity perturbations,

$$\phi_i(x, z, t) = \hat{\phi}_i(z) e^{ikx - i\omega t} \quad \text{and} \quad \eta(x, t) = \eta_0 e^{ikx - i\omega t}$$

The Laplace equations tell us that

$$\frac{d^2 \hat{\phi}_i}{dz^2} = k^2 \hat{\phi}_i \quad \Rightarrow \quad \begin{cases} \hat{\phi}_1 = A_1 e^{-kz} \\ \hat{\phi}_2 = A_2 e^{+kz} \end{cases}$$

where the solutions have been chosen so that  $\hat{\phi}_1 \rightarrow 0$  as  $z \rightarrow +\infty$  and  $\hat{\phi}_2 \rightarrow 0$  as  $z \rightarrow -\infty$ . The two boundary conditions in (5.5) then tell us that

$$-kA_1 = (-i\omega + ikU_1)\eta_0 \quad \text{and} \quad +kA_2 = (-i\omega + ikU_2)\eta_0$$

while the fact that  $\tilde{f}(t)$  in (5.6) is independent of  $x$  and  $z$  means that

$$\rho_1(-i\omega + ikU_1)A_1 = \rho_2(-i\omega + ikU_2)A_2$$

We can eliminate  $A_1$ ,  $A_2$  and  $\eta_0$  to get the quadratic in  $\omega$ ,

$$(\rho_1 + \rho_2)\omega^2 - 2k\omega(\rho_1 U_1 + \rho_2 U_2) + k^2(\rho_1 U_1^2 + \rho_2 U_2^2) = 0 \quad (5.7)$$

The roots of this quadratic give us the dispersion relation,

$$\omega = \frac{k}{\rho_1 + \rho_2} \left[ (\rho_1 U_1 + \rho_2 U_2) \pm i\sqrt{\rho_1 \rho_2} |U_1 - U_2| \right] \quad (5.8)$$

The key piece of physics is sitting in that factor of  $i$ . This is the telltale sign of an instability. To see this, we substitute this frequency into the expression (5.1) for the interface, to learn that the perturbations of the interface evolve as

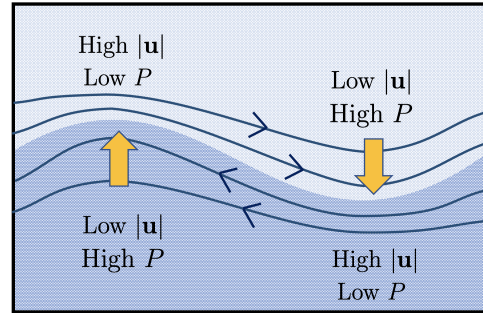
$$z = \eta(x, t) = \eta_0 \exp \left( ik \left( x - \frac{\rho_1 U_1 + \rho_2 U_2}{\rho_1 + \rho_2} t \right) \pm \frac{\sqrt{\rho_1 \rho_2}}{\rho_1 + \rho_2} |U_1 - U_2| kt \right) \quad (5.9)$$

The first term comes with an oscillatory factor of  $i$  and tells us that the disturbance propagates with velocity

$$v = \frac{\rho_1 U_1 + \rho_2 U_2}{\rho_1 + \rho_2}$$

But our real interest lies in the second term. Here there's no factor of  $i$ : the oscillatory time dependent behaviour  $e^{-i\omega t}$  becomes exponential growth or decay when  $\omega$  is complex. We learn that the perturbation grows exponentially with time. Or, more precisely, one perturbation grows and the other decays. The existence of the growing mode means that the original flow is unstable. This is the *Kevin-Helmholtz instability*.

The next question that we can ask is: why does this happen? Some intuition comes from boosting to a frame where the disturbance is stationary and then thinking about the streamlines, as shown in the figure. The streamlines of the upper fluid are more clustered together near the peaks and so, because of mass conservation, the fluid must travel faster there. Bernoulli's theorem then tells us that the pressure is smaller. But, in the trough, the streamlines are less closely packed, the fluid moves slower and so the pressure is greater.



This story is reversed for the lower fluid. The pressure is now greatest in the peak and lowest in the trough. Of course, the pressure is continuous across the interface itself — this was one of our initial boundary conditions (5.3) — but there is a pressure difference over the whole perturbation and this drives the crest upwards and the trough downwards. This is the reason for the instability.

In fact, this same effect also explains the existence of the decaying mode. If we set up a perturbation where the crest is travelling downwards, and the trough travelling up, then the pressure differences now act to decelerate the amplitude and the disturbance grows smaller over time.

### Viscosity Acts as a UV Cut-Off

For a fixed background fluid flow, the instability (5.9) grows as  $\sim e^{Ukt}$ . This means that the small wavelength modes, with  $k$  large, are more unstable. In fact, taken at face value the instability for very small wavelengths (i.e. very large  $k$ ) grows without bound. What should we make of this? Are the equations telling us that the continuum description of fluids will ultimately break down, and the interface should be thought of in terms of individual atoms?

Thankfully, no. There are (at least) two mechanisms within the continuum description that halt the runaway behaviour for large  $k$ . One of these is surface tension, and we will describe this shortly. But even in the absence of surface tension, viscosity does the job. We should replace the discontinuity in the velocity profile with an appropriate boundary layer. Our analysis above is then valid only for wavenumbers  $k \lesssim |U_1 - U_2|/\nu$ . For wavelengths smaller than this, the perturbation is stabilised by the effects of viscosity. This is a common theme in fluid dynamics, and one that we will meet again in Section 6 when we discuss turbulence: viscosity acts as a UV cut-off.

#### 5.1.2 Rolling Up The Vortex Sheet

There is another way to think about the instability, this time in terms of vorticity. If we integrate around a rectangular contour in the  $(x, z)$ -plane that crosses the interface, with sides of length  $L$  in the  $x$  direction, then the initial flow have vorticity

$$\Gamma = \oint \mathbf{u} \cdot d\mathbf{x} = (U_1 - U_2)L$$

The flows on either side of the interface are irrotational, so this vorticity must be localised at the interface itself. In the initial flow, the interface has constant vorticity per unit length. For this reason, the interface is referred to as a *vortex sheet*.

The vorticity points in the direction  $\boldsymbol{\omega} = |\boldsymbol{\omega}|\hat{\mathbf{y}}$ , where  $\hat{\mathbf{y}}$  points out of the page in the previous figures. (Note: we'll refer to the magnitude of vorticity as  $|\boldsymbol{\omega}|$  rather than  $\omega$  to avoid confusion with the frequency) and is given by

$$|\boldsymbol{\omega}| = (U_1 - U_2)\delta(z)$$

We can view the instability as a deformation of this vortex sheet. Evaluated on the linearised solution, we have

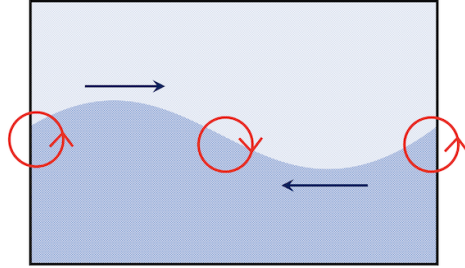
$$\begin{aligned} |\boldsymbol{\omega}| &= \left[ (U_1 - U_2) + \frac{\partial\phi_1}{\partial x} \Big|_{z=0^+} - \frac{\partial\phi_2}{\partial x} \Big|_{z=0^-} \right] \delta(z - \eta) \\ &= [(U_1 - U_2) + (-2\omega + k(U_1 + U_2))\eta_0 e^{ikx - i\omega t}] \delta(z - \eta) \end{aligned}$$

It's simplest to illustrate the physics if we restrict to the case  $\rho_1 = \rho_2$ , so that we have two identical fluids travelling at different speeds. Then, using the dispersion relation (5.8), this becomes

$$|\boldsymbol{\omega}| = [(U_1 - U_2) - i|U_1 - U_2|k\eta] \delta(z - \eta)$$

with  $\eta = \eta_0 e^{ikx - i\omega t}$  the unstable boundary. We see that, as the perturbation grows, the vorticity is no longer constant in space. It tracks the development of the interface but, because of that factor if  $i$ , is  $\pi/2$  out of phase, corresponding to  $1/4$  of a wave-length. This means that there is

no change to the vorticity at the maxima and minima, but the vorticity alternates clockwise/anti-clockwise at the midway points of the perturbation, as shown in the figure. This acts to push the crests up, and the troughs down, again



Our analysis throughout this section has been done in the linearised approximation, where the perturbation is small. However, the vortex picture gives us a good sense for what happens as the perturbation grows. If we sit in the frame where the disturbance doesn't propagate, then the upper fluid moves to the right, and the lower fluid moves to the left. The vorticity is advected in this direction, and so accumulates at the midpoint points between the peaks and troughs, shown in red in the figure. As the perturbation grows, so too does the vorticity density in this region with the result that the perturbation starts to curl around, or "roll up". The end result is the distinctive





**Figure 32.** When non-linear effects are taken into account, the Kelvin-Helmholtz instability rolls up to produce, among other things, these beautiful cloud formations.

rolling-wave feature of the Kelvin-Helmholtz instability, as shown in the cloud formation in Figure 32<sup>10</sup>.

### 5.1.3 Gravity Helps. Surface Tension Helps Too.

With our basic understanding of the instability, we can now repeat the analysis with gravity and surface tension turned on. Both manifest themselves in the boundary condition (5.6). After some algebra, the steps that previously led us to (5.7) now give

$$(\rho_1 + \rho_2)\omega^2 - 2\omega k(\rho_1 U_1 + \rho_2 U_2) + k^2(\rho_1 U_1^2 + \rho_2 U_2^2) = \gamma k^3 - gk(\rho_1 - \rho_2)$$

Solving this as a quadratic in  $\omega$  gives the dispersion relation

$$\omega = \frac{1}{\rho_1 + \rho_2} \left[ k(\rho_1 U_1 + \rho_2 U_2) \pm \sqrt{(\rho_1 + \rho_2)(\gamma k^3 + gk(\rho_2 - \rho_1)) - \rho_1 \rho_2 k^2 (U_1 - U_2)^2} \right]$$

This reduces to (5.8) when  $g = \gamma = 0$ . The presence of gravity and surface tension means that the function under the square root is no longer negative for all  $k$ . This is telling us that some wavelengths are no longer unstable, while others are.

First, suppose that have gravity  $g \neq 0$  but negligible surface tension  $\gamma = 0$ . In this case, there is an instability only if

$$k > \frac{\rho_2^2 - \rho_1^2}{\rho_1 \rho_2} \frac{g}{(U_1 - U_2)^2} \quad (5.10)$$

We see that the long wavelength (small  $k$ ) modes are no longer unstable. Heuristically, these modes are heavier and so the effect of gravity pulling them down wins over the runaway instability.

---

<sup>10</sup>and also in this [wonderful Sixty Symbols video](#).

Next suppose that we have surface tension  $\gamma \neq 0$ , but gravity is negligible so  $g = 0$ . Then there is an instability only if

$$k < \frac{\rho_1 \rho_2}{\rho_1 + \rho_2} \frac{(U_1 - U_2)^2}{\gamma} \quad (5.11)$$

This time the short wavelength (large  $k$ ) modes are stabilised. This too makes intuitive sense: the surface tension means that you pay a large cost in energy when the interface has large gradients, so small wavelength perturbations are rescued from the instability.

Alternatively, we can view (5.10) and (5.11) as conditions on how large the velocity difference  $|U_1 - U_2|$  must be to initiate an instability for a fixed  $k$ . If we have both  $g, \gamma \neq 0$  then there is no instability at all for small velocity differences. The instability only kicks in when there is some value of  $k$  such that the frequency  $\omega$  has an imaginary part. This arises when

$$(U_1 - U_2)^2 > 2 \frac{\rho_1 + \rho_2}{\rho_1 \rho_2} \sqrt{(\rho_2 - \rho_1) \gamma g}$$

Moreover, there is maximally unstable mode for which  $\omega$  has the largest imaginary value. This is the wavelength at which the instability will tend to develop.

We can do some order of magnitude estimates. For wind blowing above water, we have  $\rho_1 = \rho_{\text{air}} \approx 1 \text{ kg m}^{-3}$  and  $\rho_2 = \rho_{\text{water}} \approx 10^3 \text{ kg m}^{-3}$ . The surface tension turns out to be given by  $\gamma \approx 0.07 \text{ J m}^{-2}$ . This gives a critical wind speed of  $U_{\text{wind}} \approx 7 \text{ m s}^{-1}$ . This is the minimum speed needed to before the wind becomes responsible for making waves. It is, it turns out, in the ballpark of the average speed across the ocean. The corresponding unstable mode number is around  $k \approx 400 \text{ m}^{-1}$ , corresponding to a wavelength of a couple of centimetres. In other words, the Kelvin-Helmholtz instability due to wind causes only tiny capillary waves. The Kelvin-Helmholtz instability is not responsible for the great rolling waves on the ocean.

#### 5.1.4 The Rayleigh-Taylor Instability

There's a particularly simple application of the machinery above. We consider two fluids, now both stationary, but with the heavier one on top. It's unlikely to come as a surprise to learn that this situation is unstable. But how does the heavy fluid succeed in moving past the lighter fluid? If they're truly immiscible, then they can't just swap places. Instead, something more complicated must be going on<sup>11</sup>.

---

<sup>11</sup>Again, there is a nice demonstration on [Youtube](#).

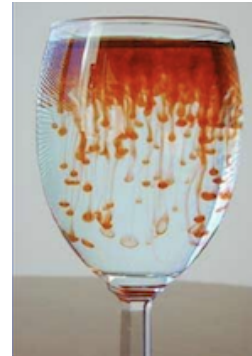
What happens is a simple form of the Kelvin-Helmholtz instability. We can trivially import our previous dispersion relation, now with  $U_1 = U_2 = 0$  and  $\rho_1 > \rho_2$ ,

$$\omega = \pm \sqrt{\frac{\gamma k^3 - gk(\rho_1 - \rho_2)}{\rho_1 + \rho_2}}$$

We see that the long wavelength modes, with  $k^2 < g(\rho_1 - \rho_2)/\gamma$  are unstable. If introduce the generalisation of the *capillary length* that we met earlier in (4.23),

$$l_c = \sqrt{\frac{\gamma}{g(\rho_1 - \rho_2)}}$$

The most unstable mode occurs for  $3k^2 = 1/l_c^2$ . This determines the size of the perturbation at which the upper layer descends into the lower. This is the *Rayleigh-Taylor instability*.



Taylor's contribution to the story above was to invoke the equivalence principle. The mathematics remains unchanged when a heavier fluid is accelerated through a lighter fluid, rather than pulled down due to gravity. This is actually a more common phenomenon, and the Rayleigh-Taylor instability describes, among other things, the mushroom clouds that appear from volcanic eruptions and nuclear explosions.

## 5.2 A Piece of Piss

We've all seen it. The stream of liquid starts out unblemished and pure. But, as it falls, ripples start to appear on the surface and these grow until the stream ultimately disintegrates into individual droplets<sup>12</sup>. This is known as the Plateau-Rayleigh instability and our goal in this section is to understand it. Fluid dynamicists refer to the stream of liquid as a *jet* and we'll adopt this terminology (although, in some contexts, that seems overly praiseworthy).



In most situations the column of liquid forms in the first place because it falls under gravity. But it will turn out that the most prominent role in the development of the

<sup>12</sup>The picture is a snapshot from [this Youtube video](#).

instability is played by surface tension. For this reason, we'll start by ignoring gravity and assuming that we are simply given a cylindrical jet, meaning a column of flowing liquid. Then, in Section 5.2.1, we'll see how gravity changes things. We ignore viscosity throughout this section.

We can go to a frame where the fluid is stationary,  $\mathbf{u} = 0$ , and with constant pressure  $P_0$ . The first question that we have to ask is: what keeps the jet together? Why doesn't the liquid just fly off in random directions? The answer is surface tension.

As we learned in Section 4.1.3, the surface tension allows for a pressure difference between the liquid and the outside air. For simplicity, we'll assume that the external pressure is vanishing. We take the jet to lie in the  $z$ -direction and have radius  $R_0$ . We use the radial coordinate  $r = \sqrt{x^2 + y^2}$  so, following (4.2), the surface is given by  $F(r) = r - R_0 = 0$ . The curvature of a circle of radius  $R_0$  is simply  $1/R_0$  so, from (4.20), the surface tension  $\gamma$  balances the pressure inside the jet when

$$P_0 = \frac{\gamma}{R_0} \quad (5.12)$$

Now we perturb. We will consider capillary surface waves that run along the jet, so that the radius is displaced by

$$R(z, t) = R_0 + \tilde{R}e^{ikz - i\omega t}$$

This means that we're anticipating wave-like behaviour. But, as in the previous section, this will be unstable if  $\omega$  is imaginary. We look for solutions in which the velocity profile and pressure have the same behaviour,

$$\mathbf{u}(\mathbf{x}, t) = [u_r(r)\hat{\mathbf{r}} + u_z(r)\hat{\mathbf{z}}]e^{ikz - i\omega t} \quad \text{and} \quad P(\mathbf{x}, t) = P_0 + \tilde{P}(r)e^{ikz - i\omega t}$$

Note that each of the perturbations is a function of the radial direction  $r$ , as well as exhibiting wave-like behaviour in the  $z$  direction.

The incompressibility condition  $\nabla \cdot \mathbf{u} = 0$  tells us that

$$\frac{1}{r} \frac{d(ru_r)}{dr} + ik u_z = 0$$

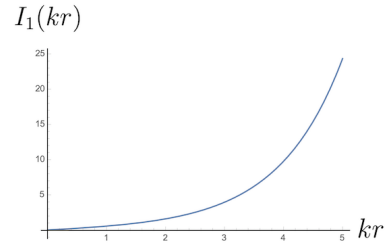
After linearising, the two components of the Euler equation are

$$-i\omega u_r = -\frac{1}{\rho} \frac{d\tilde{P}}{dr} \quad \text{and} \quad -i\omega u_z = -\frac{ik}{\rho} \tilde{P} \quad (5.13)$$

We can combine our three equations into a single, second order equation for  $u_r$ ,

$$r^2 \frac{d^2 u_r}{dr^2} + r \frac{du_r}{dr} - (1 + k^2 r^2) u_r = 0$$

This is a standard differential equation, with solutions given by the modified Bessel functions  $I_1(kr)$  and  $K_1(kr)$ . Of these,  $K_1(x)$  diverges as  $x \rightarrow 0$  and so is not appropriate for our needs. Meanwhile,  $I_1(x) \rightarrow 0$  as  $x \rightarrow 0$  but grows exponentially for large  $x$ , as shown in the figure. This is the solution for us. We learn that the radial velocity profile is given by



$$u_r(r) = VI_1(kr)$$

for some constant  $V$ . We still have two boundary conditions to impose on the surface of the jet, which is now defined by the constraint

$$F(r, z, t) = r - R(z, t) = 0$$

The first is the usual boundary condition (4.3) for a free surface, which tells us that the velocity of the fluid normal to the surface must track the surface itself. After linearisation, this gives

$$\frac{DF}{Dt} \approx \mathbf{u} \cdot \hat{\mathbf{r}} - \frac{\partial R}{\partial t} \Rightarrow V \approx -\frac{i\omega \tilde{R}}{I_1(kR_0)} \quad (5.14)$$

and determines the unknown constant  $V$  in terms of  $\omega$  and  $k$ . The second boundary condition is the requirement that the pressure is balanced by the surface tension. But now there are two contributions to the curvature of the surface. The first is because the surface is curved in the  $(x, y)$ -plane, and gives a contribution like (5.12). The second comes from the additional curvature of the form (4.20) arising from waves in the  $z$ -direction. Combining these, we have

$$P(R(t)) = P_0 + \tilde{P}(R(t))e^{ikz-i\omega t} = \frac{\gamma}{R(t)} + \gamma k^2 \tilde{R} e^{ikz-i\omega t}$$

We can linearise the  $R(t)$  terms in the second equation. We have  $\tilde{P}(R(t)) \approx \tilde{P}(R_0)$  and, by Taylor expanding,  $1/R(t) \approx 1/R_0 - (\tilde{R}/R_0^2)e^{ikz-i\omega t}$ . The terms involving just the background variables  $P_0$  and  $R_0$  cancel by virtue of (5.12), and we're left with a condition that relates the perturbation of the pressure  $\tilde{P}$  to the perturbation of the radius  $\tilde{R}$ ,

$$\tilde{P}(R_0) = \frac{\tilde{R}\gamma}{R_0^2}(k^2 R_0^2 - 1) \quad (5.15)$$

Already here we can see that there is a difference between short wavelength and long wavelength perturbations. For short wavelengths, with  $kR_0 > 1$ , the pressure increases at the surface. But for long wavelengths, with  $kR_0 < 1$ , the pressure decreases at the surface. This will turn out to be important.

We can get another expression for the pressure perturbation everywhere within the jet from the radial component of the Euler equation (5.13). This tells us that

$$\frac{d\tilde{P}}{dr} = i\omega\rho u_r = i\omega\rho V I_1(kr) \quad \Rightarrow \quad \tilde{P}(r) = \frac{i\omega\rho V}{k} I_0(kr) \quad (5.16)$$

where we've made use of the Bessel function identity  $I_1 = dI_0/dx$  to integrate the first expression. (The function  $I_0(x)$  also grows exponentially as  $x \rightarrow \infty$ , but has the value  $I_0(0) = 1$  at the origin.) Equating (5.15) and (5.16), and using our expression (5.14) for the constant  $V$ , we find

$$\omega^2 = \frac{k\gamma}{\rho R_0^2} \frac{I_1(kR_0)}{I_0(kR_0)} (k^2 R_0^2 - 1)$$

This is the dispersion relation that we were looking for. For large  $k$ , the ratio of Bessel functions is  $I_1(x)/I_0(x) \rightarrow 1$  as  $x \rightarrow \infty$  and so we get waves propagating with the dispersion  $\omega \sim k^{3/2}$ . This is the same dispersion relation that we found for surface capillary waves. (See the large  $k$  limit of (4.24).) This is to be expected: waves with a small wavelength have no knowledge of their global surrounding. They're unaware if they're sitting on a stream of liquid or on a rolling ocean.

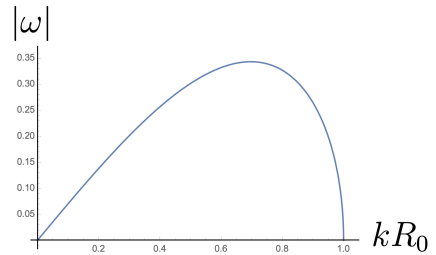
More interesting for our purposes is the long wavelength behaviour of the dispersion relation. The frequency is imaginary when

$$kR_0 < 1$$

This means that perturbations with wavelength bigger than the radius  $R_0$  of the jet will grow exponentially quickly.

The plot to right shows the function  $|\omega| \sim \sqrt{x(1-x^2)I_1(x)/I_0(x)}$  in the unstable regime, corresponding to  $0 \leq x \equiv kR_0 \leq 1$ . We see that there is a maximally unstable mode at around  $kR_0 \approx 0.7$ , corresponding to a wavelength

$$\lambda_{\max} \approx 9R_0$$



The associated time that it takes the perturbation to grow is

$$T \sim \frac{1}{|\omega|} \approx \frac{1}{0.34} \sqrt{\frac{\rho R_0^3}{\gamma}}$$

where the 0.34 is seen to be roughly the maximum of the graph. For water, with  $\rho \approx 10^3 \text{ kg m}^{-3}$  and  $\gamma \approx 0.07 \text{ J m}^{-2}$ . A stream of water from a tap has a radius of roughly  $\frac{1}{2} \text{ cm}$ , and, from the analysis above, is expected to decay in around 0.1 seconds.

### 5.2.1 Gravity Makes the Flow Thinner

We've neglected gravity in the above analysis, despite the fact that gravity is clearly responsible for the formation of the most familiar streams of liquid. We now remedy this. In fact, the most important ramification of gravity is not in the evolution of the perturbations, but in the form of the stream itself. That's what we will focus on here.

Our result is a simple application of Bernoulli's theorem that we first met in Section 2.1.4. This says that, in a gravitational field with potential  $\Phi = -\rho g z$ , the quantity

$$H = \frac{1}{2} \rho |\mathbf{u}|^2 + P - \rho g z$$

is constant. (Here we're measuring  $z$  so that it increases in a downwards direction.) Clearly we expect the component of the velocity  $U = u_z$  to increase with  $z$  simply because the fluid is being accelerated downwards. But now we have to reconcile this with the fact that the pressure must balance the surface tension as in (5.12)

$$P = \frac{\gamma}{R}$$

As we will see, this requires that both the radius  $R(z)$  and the velocity  $U(z)$  depend on  $z$ . This follows because of mass conservation, which tells us that the flux of fluid along the stream is

$$\text{Flux} = \pi R^2 U$$

and this too must be constant.

Suppose that the fluid has velocity  $U_0$  and radius  $R_0$  at  $z = 0$ . Then flux conservation gives  $R_0^2 U_0 = R(z)^2 U(z)$  and Bernoulli's principle becomes

$$\frac{1}{2} \rho U_0^2 + \frac{\gamma}{R_0} = \frac{1}{2} \rho \frac{R_0^4 U_0^2}{R(z)^4} + \frac{\gamma}{R(z)} - \rho g z$$

On rearranging,

$$R(z)^4 \left( \frac{1}{2} \rho U_0^2 + \frac{\gamma}{R_0} + \rho g z \right) - \gamma R(z)^3 - \frac{1}{2} \rho R_0^4 U_0^2 = 0 \quad (5.17)$$

In general, this has no closed form solution, although the physics is clear: as  $z$  increases,  $R(z)$  must decrease roughly as  $z^{-1/4}$ , at least for large  $z$ . There is also a limit in which we can make more progress. We define the dimensionless *Weber number* as

$$We = \frac{\rho R_0 U_0^2}{\gamma}$$

The limit of  $We \rightarrow \infty$  is where surface tension effects are no longer important. In this limit we can drop the  $\gamma$  terms in (5.17) and we have

$$R(z) = R_0 \left( 1 + \frac{2gz}{U_0^2} \right)^{-1/4}$$

where we see very clearly the advertised  $z^{-1/4}$  behaviour for large  $z$ . From our analysis of the Plateau-Rayleigh instability, we know that as the radius of the stream gets thinner, the wavelength at which the instability kicks in gets shorter.

### 5.3 Rayleigh-Bénard Convection

In this section, we will discuss fluid flows due to temperature differences. This is known as *convection*.

To start, we discuss some basics of heat. Consider a system with an energy density  $\mathcal{E}(\mathbf{x}, t)$ . We'll assume, for now, that there is no net fluid flow of the system. Nonetheless, energy can be transported from one place to another by means of *heat*. Microscopically, this describes the kinetic energy of the underlying atoms, which can be flying around in random directions even when the macroscopic fluid appears to be stationary. When energy is transported in this way, the associated continuity equation, telling us that energy is conserved, is

$$\frac{\partial \mathcal{E}}{\partial t} + \nabla \cdot \mathbf{q} = 0$$

where  $\mathbf{q}$  is the *heat flow*.

To make progress, we need a couple of results. First, at constant pressure, the change in the energy density is related to the change in the temperature  $T(\mathbf{x}, t)$  by

$$\frac{\partial \mathcal{E}}{\partial t} = c_P \frac{\partial T}{\partial t}$$



where  $c_P$  is the specific heat capacity at constant pressure. (We derived an expression for this in Section 4.4.) Second, the heat flow is related temperature difference,

$$\mathbf{q} = -\kappa \nabla T$$

with the minus sign telling us that heat flows from high temperatures to small. The coefficient  $\kappa$  is called the *thermal conductivity*. Combining these with the continuity equation, we get

$$\frac{\partial T}{\partial t} = \frac{\kappa}{c_P} \nabla^2 T \quad (5.18)$$

This is the *heat equation*.

Now we want to upgrade this description to include a background motion  $\mathbf{u}(\mathbf{x}, t)$  of the fluid. We'll focus on a thin layer of fluid, sandwiched between two plates held at different temperatures, the bottom hot and the top cold. Our expectation is that this temperature difference will drive the flow upwards and our goal is to understand how this happens.

We assume that the flow is incompressible, so

$$\nabla \cdot \mathbf{u} = 0$$

As we'll see shortly, this assumption isn't entirely innocent when we have heat conduction and we will induce a small amount of handwringing below. The generalisation of the heat equation is then straightforward: it should now be applied to parcels of fluid that are swept along with the flow, meaning

$$\frac{DT}{Dt} = \left( \frac{\partial}{\partial t} + \mathbf{u} \cdot \nabla \right) T = \frac{\kappa}{c_P} \nabla^2 T \quad (5.19)$$

We already met this equation in (4.66) when discussing sound waves. There was an additional  $\nabla \cdot \mathbf{u}$  term in (4.66) but we've set this to zero on the grounds that we're dealing with an incompressible fluid.

Our other equation is, of course, Navier-Stokes.

$$\rho \left( \frac{\partial \mathbf{u}}{\partial t} + \mathbf{u} \cdot \nabla \mathbf{u} \right) = -\nabla P - \rho(\mathbf{x}, t) g \hat{\mathbf{z}} + \mu \nabla^2 \mathbf{u} \quad (5.20)$$

We've included a gravitational force and viscosity. Both will be important for what is to come. We now have five equations (two scalar and one vector) for six unknowns:  $\mathbf{u}$ ,  $P$ ,  $\rho$  and  $T$ . We must augment these with an equation of state, relating  $\rho$ ,  $P$  and  $T$ . When discussing sound waves we relied heavily on the ideal gas equation of state. Here we are dealing with a thin layer of liquid and our equation of state will be different.

### 5.3.1 The Boussinesq Approximation

As always, we will invoke some approximation to allow us to solve the equations. This one is more subtle than most.

We start by assuming that the temperature difference between the upper and lower plate is small. Mathematically, this means that if we think of  $\rho = \rho(T)$ , then the difference in density is well approximated by a Taylor expansion

$$\rho(\mathbf{x}, t) \approx \rho_0 (1 - \alpha(T(\mathbf{x}, t) - T_0)) \quad (5.21)$$

with  $\alpha$  constant. We take  $T_0$  and  $\rho_0$  to be the temperature and density at the bottom plate. Above the plate, we expect  $T < T_0$  and so if  $\alpha > 0$ , the density will get greater as we go up. This is what we expect: increased temperature causes fluids to expand. In addition, the form (5.21) assumes that the density is independent of pressure.

At this point, it turns out that not all of our assumptions are mutually compatible! In particular, the assumption of an incompressible flow,  $\nabla \cdot \mathbf{u} = 0$ , means that mass conservation reduces to

$$\frac{\partial \rho}{\partial t} + \nabla \cdot (\rho \mathbf{u}) = 0 \quad \Rightarrow \quad \frac{D\rho}{Dt} = \frac{\partial \rho}{\partial t} + \mathbf{u} \cdot \nabla \rho = 0$$

We saw the same equation in Section 4.2 when discussing gravity waves in stratified flows. But if  $\rho$  and  $T$  are linearly related, as in (5.21), then they should solve the same equation. And the corresponding equation for temperature (5.19) has the diffusion term, proportional to  $\kappa/c_P$  on the right-hand side. In other words, incompressible flows are incompatible with heat diffusion.

Our strategy is to just bluff our way through this impasse. We will have our cake and eat it by pretending that the density  $\rho$  is actually constant. Except when it's not constant. More precisely, we will assume that the changes in density due to temperature are much smaller than the initial density  $\rho_0$ . We will make the substitution  $\rho = \rho_0$  in all places except one: the exception is the term  $g\rho$  in the Navier-Stokes equation. This is the term that will ultimately govern the physics for the simple reason that we have orchestrated a situation in which the denser, colder fluid sits on top. This means that there's a balance of forces at play in the problem, in which the heavier fluid wants to sink, but is kept afloat by the temperature gradient. It is this buoyancy force that will be important in driving the instability.

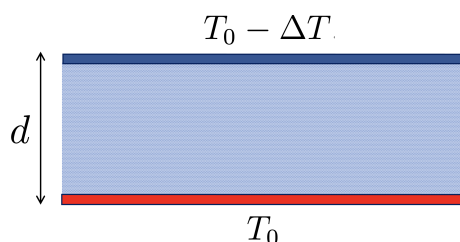
Another, perhaps more palatable, way of saying this is that we're in a situation in which the changes in the density are small, but the gravitational acceleration is large enough to make these changes important in the buoyancy force. (In addition, we use this to justify treating  $\kappa/c_P$  as constant. Recall from Section 4.4 that  $c_P$  depends on  $\rho$ , at least for an ideal gas.) This collection of ideas is known as the *Boussinesq approximation*.

Practically, this means that we work with an incompressible fluid  $\nabla \cdot \mathbf{u} = 0$  and the temperature is governed by the heat diffusion equation (5.19), while the Navier-Stokes equation becomes

$$\frac{\partial \mathbf{u}}{\partial t} + \mathbf{u} \cdot \nabla \mathbf{u} = -\frac{1}{\rho_0} \nabla P - g(1 - \alpha(T - T_0)) \hat{\mathbf{z}} + \nu \nabla^2 \mathbf{u} \quad (5.22)$$

where the kinematic viscosity is  $\nu = \mu/\rho_0$ . These are now five equations (two scalar, one vector) for five unknowns:  $\mathbf{u}$ ,  $P$  and  $T$ .

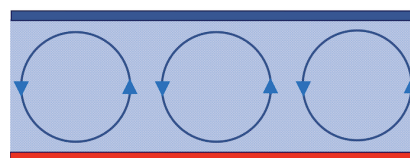
We now start by solving these equations for the heat flow between two plates. The lower plate sits at  $z = 0$  and has temperature  $T_0$ ; the upper plate sits at  $z = d$  and has temperature  $T_0 - \Delta T$ . If the plates are separated by a distance  $d$ , then there is a simple, time independent, solution to our equations with  $\mathbf{u} = 0$  and



$$T = T_0 - \Delta T \frac{z}{d} \quad \text{and} \quad P = P_0 - \rho_0 g \left( z + \frac{\alpha \Delta T}{2d} z^2 \right) \quad (5.23)$$

In this solution, the heat transfer is not due to the motion of the fluid itself. In other words, there is conduction but no convection. We would like to understand if this situation is stable against perturbations.

It turns out, unsurprisingly given the general theme of this section, that it won't be. The solution (5.23) is unstable to the fluid moving, so that heat is transferred by convection as well as conduction. The end point of this instability looks something like the situation on the right, with the fluid arranging itself into blocks known as *Bénard cells*, within each of which the fluid rises and falls<sup>13</sup>.



<sup>13</sup>A nice demonstration can be seen in this [Youtube video](#).

Before doing the full analysis, we can get some sense for why this happens. The key, as so often, is to look at the vorticity  $\boldsymbol{\omega} = \nabla \times \mathbf{u}$ . The physics is actually clearest before we make the Boussinesq approximation. We take the curl of the Navier-Stokes equation (5.20) (after dividing by the density  $\rho$ ) to get

$$\frac{\partial \boldsymbol{\omega}}{\partial t} + \mathbf{u} \cdot \nabla \boldsymbol{\omega} = \frac{1}{\rho^2} \nabla \rho \times \nabla P + \boldsymbol{\omega} \cdot \nabla \mathbf{u} + \nu \nabla^2 \boldsymbol{\omega} \quad (5.24)$$

The novelty is the first term on the right-hand side. (A similar term survives after the Boussinesq approximation if we take the curl of (5.22).) This is telling us that if the gradient of the density lies in a different direction to the gradient of pressure then it will drive a creation of vorticity. As we will see below, the perturbations that have this property give rise to the convection cells.

We can also try to figure out under what circumstances the instability will occur. Let's suppose that the width of each cell is  $d$ , the same as the height of the fluid. (At this point we're just guessing this on the grounds, but it will turn out that the size of the cell is indeed set by the depth.) We've already noted that the heavier fluid sits on top. This means that the potential energy gained if the fluid can somehow right itself is

$$\text{P.E.} \sim gd(d^3 \Delta \rho) \sim gd^4 \rho_0 \alpha \Delta T$$

But to flip over, the fluid has to overcome some viscous forces. If it flips over at speed  $U$ , then the viscous force per volume is  $\mu \nabla^2 \mathbf{u} \sim \mu U / d^2$ . This means that the actual force is  $\mu U d$  and the work done, which is  $\int F dz$ , scales as

$$\text{Work Done} \sim \mu U d^2$$

Comparing these two expressions, the gain in potential energy is sufficient to overcome the work done against viscous forces when

$$\frac{gd^2 \alpha \Delta T}{\nu U} \gg 1$$

We can also get an order of magnitude estimate for the speed  $U$  at which this takes place. From the heat equation (5.18), the time scale at which heat diffuses is  $\tau_{\text{diff}} \sim d^2 c_P / \kappa$ . Meanwhile, if the fluid flips over at speed  $U$  then it takes a time  $\tau \sim d / U$ . If we equate these we get  $U \sim \kappa / c_P d$ . The inequality above then becomes a condition on a collection of dimensionless constants

$$Ra = \frac{g \alpha c_P d^3 \Delta T}{\nu \kappa} \gg 1 \quad (5.25)$$

This is called the *Rayleigh number*. This back of the envelope analysis above suggests that we will find an instability when  $Ra \gg 1$ . We'll see that this is confirmed in our subsequent analysis.

### 5.3.2 Perturbation Analysis

We will perturb the background solution (5.23), turning on a velocity field  $\mathbf{u}$  together with temperature and pressure perturbations that we denote as  $\delta T(\mathbf{x}, t)$  and  $\delta P(\mathbf{x}, t)$  respectively. These will all be considered small in the sense that we will linearise the equations of motion. The temperature equation (5.19) becomes

$$\frac{\partial \delta T}{\partial t} - \frac{\Delta T}{d} u_z = \frac{\kappa}{c_P} \nabla^2 \delta T \quad (5.26)$$

and the Navier-Stokes equation becomes

$$\frac{\partial \mathbf{u}}{\partial t} = -\frac{1}{\rho_0} \nabla \delta P + g \alpha \delta T \hat{\mathbf{z}} + \nu \nabla^2 \mathbf{u} \quad (5.27)$$

Meanwhile, the velocity perturbations remain incompressible,  $\nabla \cdot \mathbf{u} = 0$ .

### Dimensional Analysis

We can illustrate the physics in these equations if we write them in terms of dimensionless variables. For this, we'll need to rescale both space and time as

$$\tilde{\mathbf{x}} = \frac{\mathbf{x}}{d} \quad \text{and} \quad \tilde{t} = \frac{\kappa}{c_P d^2} t$$

This means, in particular, that our lower and upper boundaries are at  $\tilde{z} = 0$  and  $\tilde{z} = 1$  respectively. We also rescale our dynamical variables

$$\tilde{T} = \frac{\delta T}{\Delta T} \quad , \quad \tilde{P} = \frac{c_P d^2}{\kappa^2 \rho_0} \delta P \quad , \quad \tilde{\mathbf{u}} = \frac{c_P d}{\kappa} \mathbf{u}$$

Then the temperature perturbation equation (5.26) becomes

$$\frac{\partial \tilde{T}}{\partial \tilde{t}} - \tilde{u}_z = \tilde{\nabla}^2 \tilde{T} \quad (5.28)$$

while the perturbed Navier-Stokes equation (5.27) exhibits two dimensionless coefficients.

$$\frac{\partial \tilde{\mathbf{u}}}{\partial \tilde{t}} = -\tilde{\nabla} \tilde{P} + Ra Pr \tilde{T} \hat{\mathbf{z}} + Pr \tilde{\nabla}^2 \tilde{\mathbf{u}} \quad (5.29)$$

The first of these is the Rayleigh number  $Ra$  that we already met in (5.25). The second is the *Prandtl number*,

$$Pr = \frac{c_P \nu}{\kappa}$$

Unlike most of our other dimensionless numbers, the Prandtl number is a property only of the liquid, not of the flow. It has the value  $Pr \approx 0.7$  for air and for most gases. It is  $Pr \approx 7.5$  for water at room temperature.

Our goal is to solve (5.28) and (5.29) subject to suitable boundary conditions. Clearly we require  $\tilde{u}_z = 0$  at  $\tilde{z} = 0$  and  $\tilde{z} = 1$  so that nothing flows into either plate. Also  $\tilde{T} = 0$  at  $\tilde{z} = 0$  and  $\tilde{z} = 1$  as the plates are at a fixed temperature.

In addition, it is natural to impose the no-slip boundary condition on both plates, since our liquid is viscous. It may be natural, but we're not going to do it. The reason is simply laziness! The calculation below is challenging enough and by the time we get to solve the equations life is much easier if we impose the somewhat unphysical requirement that there is no stress on the plate, meaning

$$\frac{\partial \tilde{u}_x}{\partial \tilde{z}} = \frac{\partial \tilde{u}_y}{\partial \tilde{z}} = 0 \quad \text{at} \quad \tilde{z} = 0, 1$$

In fact it turns out that this is the correct boundary condition to impose on a free surface, rather than a rigid plate. As we'll see (in the discussion following (5.37)), to do the calculation we really need a boundary condition on  $\tilde{u}_z$ . We get this by writing the boundary condition above as

$$\frac{\partial}{\partial \tilde{z}} \left( \frac{\partial \tilde{u}_x}{\partial \tilde{x}} + \frac{\partial \tilde{u}_y}{\partial \tilde{y}} \right) = 0 \quad \Rightarrow \quad \frac{\partial^2 \tilde{u}_z}{\partial \tilde{z}^2} = 0 \quad \text{at} \quad \tilde{z} = 0, 1 \quad (5.30)$$

where we've invoked the incompressibility condition  $\tilde{\nabla} \cdot \tilde{\mathbf{u}} = 0$ .

### You May Wish To Roll Up Your Sleeves

To proceed, we first take the curl of (5.29) to get

$$\frac{\partial \tilde{\boldsymbol{\omega}}}{\partial \tilde{t}} = Ra Pr \tilde{\nabla} \tilde{T} \times \hat{\mathbf{z}} + Pr \tilde{\nabla}^2 \tilde{\boldsymbol{\omega}}$$

where  $\tilde{\boldsymbol{\omega}} = \tilde{\nabla} \times \tilde{\mathbf{u}}$ . Curiously, it turns out that the best way to proceed is to take yet another curl. This then gives

$$\frac{\partial \tilde{\nabla}^2 \tilde{\mathbf{u}}}{\partial \tilde{t}} = Ra Pr \left( \hat{\mathbf{z}} \tilde{\nabla}^2 \tilde{T} - \tilde{\nabla} \left( \frac{\partial \tilde{T}}{\partial \tilde{z}} \right) \right) + Pr \tilde{\nabla}^4 \tilde{\mathbf{u}}$$

where we've used  $\tilde{\nabla} \times (\tilde{\nabla} \times \tilde{\mathbf{u}}) = -\tilde{\nabla}^2 \tilde{\mathbf{u}}$  for an incompressible flow with  $\tilde{\nabla} \cdot \tilde{\mathbf{u}} = 0$ . This is now fourth order in spatial derivatives. We'll focus on the  $z$ -component, which is

$$\frac{\partial \tilde{\nabla}^2 \tilde{u}_z}{\partial \tilde{t}} = Ra Pr \left( \frac{\partial^2 \tilde{T}}{\partial \tilde{x}^2} + \frac{\partial^2 \tilde{T}}{\partial \tilde{y}^2} \right) + Pr \tilde{\nabla}^4 \tilde{u}_z \quad (5.31)$$

This is to be solved in conjunction with the temperature equation (5.28).

We'll look for solutions using separation of variables. Furthermore, we'll anticipate the instability by looking for solutions that grow exponentially in time as  $e^{\Gamma \tilde{t}}$ ,

$$\tilde{u}_z(\mathbf{x}, t) = V(\tilde{z}) X(\tilde{x}, \tilde{y}) e^{\Gamma \tilde{t}} \quad \text{and} \quad \tilde{T}(\mathbf{x}, t) = \theta(\tilde{z}) X(\tilde{x}, \tilde{y}) e^{\Gamma \tilde{t}} \quad (5.32)$$

Note that we've assumed that both the velocity field and temperature have the same spatial dependence  $X(x, y)$  in the  $x$  and  $y$  directions. With this ansatz, the temperature equation (5.28) becomes

$$\frac{1}{\theta} \left[ \frac{d^2 \theta}{d\tilde{z}^2} - \Gamma \theta + V \right] = -\frac{1}{X} \left[ \frac{\partial^2 X}{\partial \tilde{x}^2} + \frac{\partial^2 X}{\partial \tilde{y}^2} \right] \quad (5.33)$$

Now, the left-hand side depends only on  $\tilde{z}$  and the right-hand side depends only on  $\tilde{x}$  and  $\tilde{y}$ , which means that both sides must actually be constant. For the solution to be bounded in the  $x$  and  $y$  directions, this constant should be positive. We'll call it  $K^2$ . We then have

$$\tilde{\nabla}_2^2 X \equiv \frac{\partial^2 X}{\partial \tilde{x}^2} + \frac{\partial^2 X}{\partial \tilde{y}^2} = -K^2 X \quad \Rightarrow \quad X(\tilde{x}, \tilde{y}) \sim e^{iK_x \tilde{x} + iK_y \tilde{y}} \quad (5.34)$$

where  $K^2 = K_x^2 + K_y^2$ . We already start to see the ripples forming in the  $(x, y)$ -plane. Reverting back to dimensionful coordinates, we see that these ripples will have wavelength  $\lambda = 2\pi d/K$  and so the constant  $K$  is simply the (magnitude of the) dimensionless wavenumber.

Our next task is to relate  $K$  to the instability constant  $\Gamma$ . This ultimately comes from equating the left-hand side of (5.33) to the same constant,

$$\left( \frac{d^2}{d\tilde{z}^2} - \Gamma - K^2 \right) \theta = -V \quad (5.35)$$

This equation relates the temperature profile  $\theta(\tilde{z})$  to the velocity profile  $V(\tilde{z})$ .

We can get another equation relating these variables by substituting the same ansatz (5.32) into the Navier-Stokes equation (5.31). We replace  $\tilde{\nabla}_2^2 X$  with the expression (5.34) to get

$$\Gamma \left( \frac{d^2}{d\tilde{z}^2} - K^2 \right) V = -Ra Pr K^2 \theta + Pr \left( \frac{d^2}{d\tilde{z}^2} - K^2 \right)^2 V \quad (5.36)$$

We can eliminate  $\theta$  in this equation using (5.35). To do this, we have to act with  $(d^2/d\tilde{z}^2 - \Gamma - K^2)$ . We have

$$\left( \frac{d^2}{d\tilde{z}^2} - K^2 \right) \left( \frac{d^2}{d\tilde{z}^2} - \Gamma - K^2 \right) \left( \Gamma - Pr \left( \frac{d^2}{d\tilde{z}^2} - K^2 \right) \right) V = Ra Pr K^2 V \quad (5.37)$$

Good? Good. After all of this, we're left with a sixth order differential equation. Sometimes, physics just isn't pretty.

We want to solve this subject to the boundary condition  $V = 0$  and, from (5.30),  $d^2V/d\tilde{z}^2 = 0$  at the two boundaries  $\tilde{z} = 0, 1$ . We also require  $\theta = 0$  at  $\tilde{z} = 0, 1$  and, from (5.36), we can see that this is only consistent if, in addition, we require  $d^4V/d\tilde{z}^4 = 0$  at the boundaries. This means that we must solve (5.37) subject to the six boundary conditions

$$V = \frac{d^2V}{d\tilde{z}^2} = \frac{d^4V}{d\tilde{z}^4} = 0 \quad \text{at} \quad \tilde{z} = 0, 1 \quad (5.38)$$

This, as we shall now see, isn't so bad.

Before we do the thing that isn't so bad, it's worth pausing to reconsider these boundary conditions. Recall that the condition (5.30) was born more out of sloth than physical necessity. With a rigid boundary, it would have been more appropriate to impose the no-slip condition which leads to the requirement  $dV/d\tilde{z} = 0$  at the boundaries rather than  $d^2V/d\tilde{z}^2 = 0$ . It turns out that we have to work harder to find such solutions.

Returning to the boundary conditions (5.38), the solutions are simply sine functions

$$V(\tilde{z}) = \sin(n\pi\tilde{z})$$

with  $n \in \mathbb{Z}$ . The somewhat daunting looking equation (5.37) then becomes the algebraic condition

$$(n^2\pi^2 + K^2)(n^2\pi^2 + \Gamma + K^2)\left(n^2\pi^2 + K^2 + \frac{\Gamma}{Pr}\right) = Ra K^2 \quad (5.39)$$

This is the analog of our previous dispersion relations, now telling us how the characteristic (inverse) time of the instability,  $\Gamma$ , relates to the wavelength. For some fixed  $n \in \mathbb{Z}$ , there is clearly a solution to this equation with  $\Gamma > 0$  when the Rayleigh number is sufficiently large,

$$Ra > \frac{(n^2\pi^2 + K^2)^3}{K^2} \quad (5.40)$$

This confirms that intuition that we saw previously that the instability should only kick in when  $Ra$  is big enough.

The smallest value of  $Ra$  for which there is a solution occurs when  $n = 1$ . In this case, we minimise the function above

$$\frac{d}{dK^2} \left[ \frac{(n^2\pi^2 + K^2)^3}{K^2} \right] = 0 \quad \Rightarrow \quad K^2 = \frac{\pi^2}{2}$$



From our previous discussion, this corresponds to the formation of a cell with size  $\sim 2\sqrt{2}d$ . Plugging this value back into (5.40), we have an instability provided that

$$Ra > \frac{27\pi^4}{4} \approx 660$$

For values of  $Ra$  just above this number, only the  $n = 1$  mode is unstable. As  $Ra$  increases, more and more  $K$  modes become unstable as well as mode of higher  $n$ . As usual, the most unstable mode is that with largest  $\Gamma$  and this determines the preferred choice of  $K$ .

## 5.4 Instabilities of Inviscid Shear Flows

In this section, we turn our attention to instabilities of shear flows. That is, flows that takes the form

$$\mathbf{u}(\mathbf{x}, t) = U(z)\hat{\mathbf{x}}$$

together with some pressure field  $P(\mathbf{x})$ . We'll consider this velocity field over some finite width,

$$-h \leq z \leq +h$$

with suitable boundary conditions imposed on the edges  $z = \pm h$ . Both Couette flow and Poiseuille flow described in Section 3.2 are of this form. Our goal is to understand when instabilities of such flows may arise. We'll make progress, albeit limited. In particular, it turns out that we will not be able to demonstrate instability of either of these basic flows, even though they both unstable at suitably high Reynolds number. We will, however, be able to understand why this is a difficult problem!

We give the shear flow a nudge with perturbations of the form

$$\mathbf{u}(\mathbf{x}, t) = U(z)\hat{\mathbf{x}} + \tilde{\mathbf{u}}(z)e^{ik_x x + ik_y y - i\omega t}$$

together with some perturbation of the pressure

$$\delta P(\mathbf{x}) = \rho \tilde{P}(z)e^{ik_x x + ik_y y - i\omega t}$$

Note that we've included a factor of  $\rho$  on the right-hand side to ensure that later equations are a little simpler. It does mean, however, that  $\tilde{P}$  does not have the dimensions of pressure.

As in our previous examples, we take the wavenumbers  $k_x$  and  $k_y$  to be some fixed real numbers and we choose them to be positive,  $k_x, k_y > 0$ . We then use the equations of motion to determine  $\omega$ . In general,  $\omega$  can be complex (as, indeed, can  $\tilde{u}_z$  and  $\tilde{P}_z$ ), and an instability occurs when we find  $\text{Im } \omega > 0$ . We will now derive some general statements about when the original flow is unstable.

We first met shear flows when we introduced viscosity in Section 3, with the shear induced by the no-slip boundary condition. Nonetheless, we will first study instabilities in the context of the Euler equation,

$$\frac{\partial \mathbf{u}}{\partial t} + \mathbf{u} \cdot \nabla \mathbf{u} = -\frac{1}{\rho} \nabla P$$

We'll then add viscosity to the discussion in Section 5.5. The linearised perturbation equations read

$$i(k_x U - \omega) \tilde{u}_x + \tilde{u}_z \frac{dU}{dz} = -ik_x \tilde{P} \quad (5.41)$$

$$i(k_x U - \omega) \tilde{u}_y = -ik_y \tilde{P} \quad (5.42)$$

$$i(k_x U - \omega) \tilde{u}_z = -\frac{d\tilde{P}}{dz} \quad (5.43)$$

These should be augmented with the incompressibility condition

$$ik_x \tilde{u}_x + ik_y \tilde{u}_y + \frac{d\tilde{u}_z}{dz} = 0 \quad (5.44)$$

We've allowed for wavelike perturbations in both the  $x$  and  $y$ -directions and a general perturbation in the  $z$ -direction. In fact, if we're looking for the onset of instabilities then we can ignore motion in the  $y$ -direction and focus just on the two-dimensional setting. This follows from:

**Squire's Theorem:** Perturbations in the  $y$ -direction do not induce further instabilities of the flow.

**Proof:** Define a velocity in the diagonal direction in the  $(x, y)$ -plane by

$$v = \frac{1}{K} (k_x \tilde{u}_x + k_y \tilde{u}_y) \quad \text{with} \quad K^2 = k_x^2 + k_y^2$$

We can combine (5.41) and (5.42) into the equation

$$i(KU - \omega')v + \tilde{u}_z \frac{dU}{dz} = -iK \tilde{P}' \quad (5.45)$$

where the primes do not denote derivatives but, instead, are a rescaled frequency and a rescaled pressure perturbation,

$$\omega' = \frac{K}{k_x} \omega \quad \text{and} \quad \tilde{P}' = \frac{K}{k_x} \tilde{P}$$

In terms of these rescaled variables, the perturbation equation (5.43) in the  $z$ -direction and the incompressibility condition (5.44) become

$$i(KU - \omega')\tilde{u}_z = -\frac{d\tilde{P}'}{dz} \quad \text{and} \quad iKv + \frac{d\tilde{u}_z}{dz} = 0 \quad (5.46)$$

Equations (5.45) and (5.46) describe an effective 2d system, with various quantities rescaled as above. In particular, the frequency is rescaled so that  $|\omega'| > |\omega|$ . But, as in previous examples, the question of whether the flow is unstable will boil down to whether the imaginary part of the frequency is non-zero. Clearly, we have  $\text{Im } \omega' \neq 0$  whenever  $\text{Im } \omega \neq 0$ . The fact that  $|\omega'| > |\omega|$  tells us that the growth of instability is faster in the  $v$  direction, but doesn't change when the instability kicks in.  $\square$

#### 5.4.1 Rayleigh's Criterion

Because our interest will lie in identifying the conditions under which flows are unstable, Squire's theorem affords us the option of simplifying the situation by setting  $\tilde{u}_y = k_y = 0$ . We'll also take this opportunity to write  $k_x = k$ . This leaves us with the perturbation equations (5.41), (5.43) and (5.44). We can eliminate  $\tilde{u}_x$  using the incompressibility condition (5.44), leaving us with two equations

$$\begin{aligned} -\left(U - \frac{\omega}{k}\right) \frac{d\tilde{u}_z}{dz} + \tilde{u}_z \frac{dU}{dz} &= -ik\tilde{P} \\ i(kU - \omega)\tilde{u}_z &= -\frac{d\tilde{P}}{dz} \end{aligned}$$

Next, we can eliminate the pressure perturbation at the expense of differentiating the first of the equations above. In doing so, there are two terms of the form  $(dU/dz)(d\tilde{u}_z/dz)$  that cancel and we are left with a simple, second order differential equation for  $\tilde{u}_z$ ,

$$\left[ \left( U - \frac{\omega}{k} \right) \left( \frac{d^2}{dz^2} - k^2 \right) - \frac{d^2 U}{dz^2} \right] \tilde{u}_z = 0 \quad (5.47)$$

This is the *Rayleigh equation*. Our goal is to solve this equation for a given background flow  $U(z)$  and wavenumber  $k$ , subject to the boundary condition  $\tilde{u}_z = 0$  at  $z = \pm h$ , which ensures that the perturbations don't flow into the edges of the channel. The solution contains both the profile of the boundary perturbation  $\tilde{u}_z$  as well as the corresponding frequency  $\omega$ .

We'd like to know when solutions to the Rayleigh equation (5.47) have  $\text{Im}(\omega) \neq 0$ , signalling an instability. One possibility is to simply pick a choice of initial flow  $U(z)$  and solve the eigenvalue equation (5.47). That is often hard. Here, instead, we derive some simple, general conditions that any flow must obey if it is to have a linear instability.

We write the Rayleigh equation as

$$\frac{d^2 \tilde{u}_z}{dz^2} - k^2 \tilde{u}_z - \frac{U''}{U - \omega/k} \tilde{u}_z = 0$$

We now multiply both sides by the complex conjugate of the velocity perturbation,  $\tilde{u}_z^*$  and integrate across the width of flow in the  $z$ -direction. After integrating by parts, and using the boundary condition  $\tilde{u}_z = 0$  at  $z = \pm h$ , we have

$$\int_{-h}^{+h} dz \left( \left| \frac{d\tilde{u}_z}{dz} \right|^2 + k^2 |\tilde{u}_z|^2 \right) = - \int_{-h}^{+h} dz \frac{U''}{U - \omega/k} |\tilde{u}_z|^2 \quad (5.48)$$

The left-hand side is real and positive. This means that the imaginary part of the right-hand side must vanish. The only complex quantity on the right-hand side is the frequency  $\omega$ , so this tells us

$$\text{Im} \left[ \int_{-h}^{+h} dz \frac{U''}{U - \omega/k} |\tilde{u}_z|^2 \right] = \frac{\text{Im}(\omega)}{k} \int_{-h}^{+h} dz \frac{U''}{|U - \omega/k|^2} |\tilde{u}_z|^2 = 0$$

How can this equation be satisfied? One obvious way is if  $\text{Im}(\omega) = 0$ , in which case the flow is stable. But they're not the perturbations that we care about. Instead, we're interested in situation in which  $\text{Im}(\omega) \neq 0$  and the flow is unstable. This can only happen if

$$\int_{-h}^{+h} dz \frac{U''}{|U - \omega/k|^2} |\tilde{u}_z|^2 = 0 \quad (5.49)$$

But both  $|\tilde{u}_z|^2$  and the denominator are manifestly positive. The only possible way that the equality can hold is if  $U''$  changes sign at some value of  $-h < z < h$ , so that it is positive in some region of the flow and negative in others. This means that there must be an inflection point,

$$\frac{d^2 U}{dz^2} = 0 \quad \text{for some } -h < z < h$$

This is the *Rayleigh criterion* for linear instability of an inviscid flow. It is not a sufficient criterion. But it is necessary.

### 5.4.2 Fjortoft's Criterion

There is more that we can say about the condition for instability, at least under certain circumstances. Our equation (5.48) tells us that

$$\operatorname{Re} \left[ \int_{-h}^{+h} dz \frac{U''}{U - \omega/k} |\tilde{u}_z|^2 \right] < 0 \quad \Rightarrow \quad \int_{-h}^{+h} dz \frac{U''(U - \operatorname{Re}(\omega)/k)}{|U - \omega/k|^2} |\tilde{u}_z|^2 < 0$$

If there is an instability, then (5.49) must hold and this means that the  $\operatorname{Re}(\omega)$  term in the above expression actually vanishes when integrated over the width of the channel. So we actually have the requirement

$$\int_{-h}^{+h} dz \frac{U''U}{|U - \omega/k|^2} |\tilde{u}_z|^2 < 0 \quad (5.50)$$

It's not immediately obvious that this buys us anything beyond the Rayleigh criterion. This is because we have little information about most of the variables in the equation (5.50). We assume that we're given some starting flow  $U(z)$  and we're searching for a perturbation with some fixed wavenumber  $k$ . But both  $\omega$  and  $\tilde{u}_z$  are fixed by the Rayleigh equation (5.47) that we haven't yet solved. In particular, for a given  $k$  it may well be that  $\tilde{u}_z$  is peaked at some value of  $z$ , but we have no idea where. So it's difficult to see what new information can be buried in the inequality (5.50)

Nonetheless, there's a clever trick that does allow us to extract more information from (5.50). The equation (5.48) that previously allowed us to drop the  $\operatorname{Re}(\omega)$  term from the integral also allows us to add any other constant to the numerator, so we can equally well write (5.50) as

$$\int_{-h}^{+h} dz \frac{U''(U - U_*)}{|U - \omega/k|^2} |\tilde{u}_z|^2 < 0 \quad (5.51)$$

for any constant  $U_*$  of our choice. At this point, we need two further assumptions to make progress. We assume that:

- There is just a single Rayleigh inflection point at  $z = z_*$ .
- The background flow  $U(z)$  is monotonically increasing, so  $U'(z) \geq 0$  for all  $z$ .

With these two assumptions, we take  $U_* = U(z_*)$ . Together with the assumption of monotonicity of  $U$ , this ensures that the factor  $(U - U_*)$  flips sign at  $z = z_*$ . This, of course, is the same place that  $U''(z)$  flips sign so, for this particular choice, the product  $U''(U - U_*)$  has the same sign for all values of  $z$ . The inequality (5.50) tells us that this sign must be negative:

$$U''(U - U_*) \leq 0 \quad \forall z$$

with equality only when  $z = z_*$ . This is the *Fjortoft criterion*.

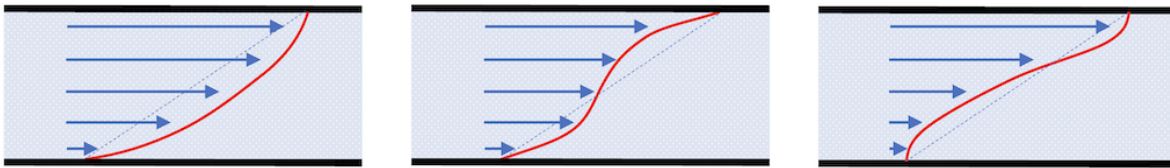


**Figure 33.** The first flow is stable by Rayleigh, the second by Fjortoft. Only the third may be unstable.

We can also phrase this criterion in terms of the vorticity of the background flow,  $\omega = \nabla \times \mathbf{u}$ , whose magnitude is

$$|\omega| = \Omega = \frac{dU}{dz}$$

The Rayleigh criterion tells us that there is a point in the flow where the vorticity is stationary, with  $d\Omega/dz = 0$ . The Fjortoft criterion tells us that, away from this inflection point,

$$\frac{d\Omega}{dz}(U - U_\star) < 0 \quad (5.52)$$

Suppose that, away from this point,  $U'(z) > 0$  so that  $\Omega > 0$ . Then for  $z < z_\star$  we have  $U - U_\star < 0$  and (5.52) tells us that  $\Omega$  is increasing. Similarly, for  $z > z_\star$ , (5.52) says that the vorticity  $\Omega$  must be decreasing. In other words, the Fjortoft criterion is telling us that, for a flow to be unstable, the vorticity  $\Omega$  must have a *maximum* at  $z = z_\star$ . The same conclusion is reached if  $U'(z) < 0$ : the magnitude of the vorticity  $|\Omega|$  must have a maximum for the flow to be unstable.

Three examples of shear flows are shown in Figure 33. The first has no point where  $U''(z) = 0$  and so is stable by the Rayleigh criterion. The second has an inflection point but the vorticity is a minimum there: it is stable by the Fjortoft criterion. The third has a point where the vorticity is maximum and obeys both criterion. Only this one may have a linear instability. (And even then, it is not guaranteed. Our conditions are sufficient, not necessary.)

You might have noticed that our original Poiseuille flow of Section 3.2 is stable according to the Rayleigh criterion, with  $U''(z) < 0$  everywhere. That's something of a surprise because we showed photographs in Figure 30 of Poiseuille flow disintegrating as the Reynolds number is cranked up. But the Rayleigh and Fjortoft criteria apply only to inviscid flows and it turns out that to fully understand instabilities we need to

include the effects of viscosity. We'll turn to this in Section 5.5. (The Couette flow is something of a special case since it has  $U''(z) = 0$  everywhere and we'll consider it separately in Section 5.4.4.)

### 5.4.3 Howard's Semi-circle Theorem

There's yet more information to be extracted from the Rayleigh equation. To do this, we make the change of variables that combines the perturbation  $\tilde{u}_z$  with the background flow  $U$ ,

$$V = \frac{\tilde{u}_z}{U - \omega/k}$$

We should be a little careful because it may be that the new variable  $V$  is ill-defined if, for some value of  $z$ , we have  $U(z) = \omega/k$ . Clearly, however, this will not be a problem if we have an unstable perturbation with  $\omega$  complex because  $U(z)$  is real.

The Rayleigh equation (5.47) is

$$\left[ (U - \omega/k) \left( \frac{d^2}{dz^2} - k^2 \right) - \frac{d^2 U}{dz^2} \right] (U - \omega/k) V = 0$$

After expanding out, this becomes

$$(U - \omega/k)^2 \frac{d^2 V}{dz^2} + 2(U - \omega/k) \frac{dU}{dz} \frac{dV}{dz} - k^2 (U - \omega/k)^2 V = 0$$

which we can then write as

$$\frac{d}{dz} \left[ \left( U - \frac{\omega}{k} \right)^2 \frac{dV}{dz} \right] - k^2 \left( U - \frac{\omega}{k} \right)^2 V = 0$$

Now we play the same trick as before: we multiply by the complex conjugate  $V^*$  and integrate over the width of the flow. After integrating by parts, and using the boundary condition  $\tilde{u}_z = 0$  at  $z = \pm h$ , we have

$$\int_{-h}^{+h} dz \left( U - \frac{\omega}{k} \right)^2 Q = 0 \quad \text{with} \quad Q = \left| \frac{dV}{dz} \right|^2 + k^2 |V|^2 \quad (5.53)$$

Clearly the quantity  $Q$  is non-negative for all  $z$ . If the flow is unstable then  $\text{Im}(\omega) \neq 0$ , and the imaginary part of the equation is

$$\frac{2\text{Im}(\omega)}{k} \int_{-h}^{+h} dz \left( U - \frac{\text{Re}(\omega)}{k} \right) Q = 0 \quad (5.54)$$

So the quantity in brackets must change sign. This is only possible if

$$kU_{\min} < \text{Re}(\omega) \leq kU_{\max}$$

This can also be viewed as a bound on the phase velocity of the disturbance,  $c = \text{Re}(\omega)/k$ . The phase velocity is bounded by the velocities of the background flow:  $U_{\min} < c < U_{\max}$ .

The real part of (5.53) reads

$$\int_{-h}^{+h} dz \left( (Uk - \text{Re}(\omega))^2 - \text{Im}(\omega)^2 \right) Q = 0 \quad (5.55)$$

There's a way to massage this into something more useful by removing the explicit factors of  $U$  in the integrand. To remove the term quadratic in  $U$ , we make use of the trivial fact that  $(U - U_{\min})(U_{\max} - U) \geq 0$ , so we have

$$\int_{-h}^{+h} dz (U - U_{\min})(U_{\max} - U)k^2 Q \geq 0 \quad (5.56)$$

Adding (5.55) and (5.56), and using (5.57), we have

$$\int_{-h}^{+h} dz \left( Uk \left( -2\text{Re}(\omega) + k(U_{\max} - U_{\min}) \right) + \text{Re}(\omega)^2 - \text{Im}(\omega)^2 - U_{\max}U_{\min}k^2 \right) Q \geq 0$$

But we can remove terms linear in  $U$  since, by (5.54), we have

$$\int_{-h}^{+h} dz Uk Q = \int_{-h}^{+h} dz \text{Re}(\omega) Q \quad (5.57)$$

The upshot is that we get the inequality

$$\int_{-h}^{+h} dz \left( \text{Re}(\omega)^2 + \text{Im}(\omega)^2 - \text{Re}(\omega)(U_{\max} - U_{\min})k + U_{\max}U_{\min}k^2 \right) Q \leq 0$$

Clearly the object in brackets must be negative, meaning that the real and imaginary parts of the frequency are bounded by

$$\left( \text{Re}(\omega) - \frac{k}{2}(U_{\max} - U_{\min}) \right)^2 + \text{Im}(\omega)^2 \leq \frac{k^2}{4} (U_{\max} + U_{\min})^2$$

This is *Howard's semi-circle theorem*. It puts a bound on the instability in the complex  $\omega$  plane in the form of a semi-circle as shown in Figure 34. In particular, this condition gives a bound on the growth rate  $\text{Im}(\omega)$  of the instability.



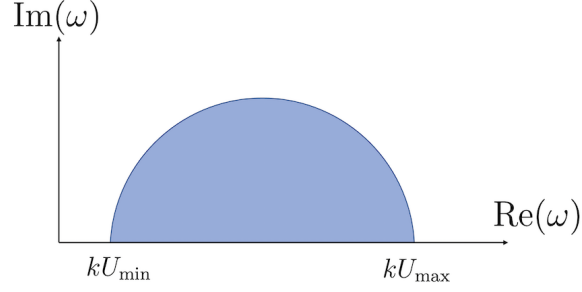


**Figure 34.** The range of allowed unstable behaviour in the complex  $\omega$  plane.

#### 5.4.4 Couette Flow Revisited

Couette flow is special because, as we saw in Section 3.2, the velocity field is linear:  $U(z) \sim z$ . This means that  $U''(z) = 0$  for all  $z$  and the Rayleigh criterion (5.49) appears to be toothless. Which leads us to ask: is the flow actually unstable?

In this case, the background flow is simple enough that we can just go ahead and solve the equations. The Rayleigh equation (5.47) reads

$$\left(\alpha z - \frac{\omega}{k}\right) \left(\frac{d^2}{dz^2} - k^2\right) \tilde{u}_z = 0 \quad (5.58)$$

where we've taken the background flow to be  $U(z) = \alpha z$  for constant  $\alpha$ . If we look for smooth solutions then the background perturbation must be given by

$$\left(\frac{d^2}{dz^2} - k^2\right) \tilde{u}_z = 0 \quad \Rightarrow \quad \tilde{u}_z = A \sinh k(z - z_0)$$

But we still need to impose the boundary condition  $\tilde{u}_z = 0$  at  $z = \pm h$ . And that can only hold if  $A = 0$ .

This is a little confusing! It seems to be telling us that there can be no perturbations of Couette flow, stable or otherwise. But that doesn't sound right. What if you splash it?! Surely something must happen. What?

In fact, to find perturbations we must relax the condition that  $\tilde{u}_z$  is smooth. Suppose that we admit the solution

$$\tilde{u}_z = \begin{cases} A_+ \sinh k(z - h) & z > z_c \\ A_- \sinh k(z + h) & z < z_c \end{cases}$$

This immediately satisfies the boundary condition requirement  $\tilde{u}_z = 0$ . We still need the velocity perturbation to be continuous, even if it's not differentiable, and this imposes the condition

$$A_+ \sinh k(z_c - h) = A_- \sinh k(z_c + h)$$

This should be thought of as fixing, say  $A_+$ , in terms of  $A_-$  given the position  $z_c$  of the jump.

How worried should we be about the discontinuity? The derivative in the Rayleigh equation (5.58) will certainly hit it, giving infinity. But we can rescue the situation if the pre-factor vanishes. This holds if the frequency  $\omega$  is given by

$$\omega = \alpha z_c k$$

This is rather nice. We find that we have a continuous spectrum of stable, wavelike modes, with the discontinuity propagating at the same phase velocity as the background flow at that point,  $\omega/k = \alpha z_c = U(z_c)$ .

The modes that we have found are marginal, in the sense that they neither grow nor decay with time. But we've only looked at first order in perturbation theory and it may well be that higher order corrections change the story. Although we will not show it here, it turns out that these marginal modes are not rendered unstable by higher order terms. Nor are they unstable when we include viscosity. Couette flow is stable to arbitrarily small perturbations.

However, that doesn't mean that Couette flow is actually stable! Experiment and numerics show that the Couette flow is actually unstable, and develops turbulence for  $Re \gtrsim 400$ . The instability arises due to perturbations of some finite amplitude.

## 5.5 Instabilities of Viscous Shear Flows

In this section, we'll repeat the analysis of the stability of shear flows, this time with viscosity added.

The set-up is the same as in Section 5.4, with a flow over a finite width  $|z| \leq h$ , with suitable boundary conditions (such as no-slip) imposed on the edges. The initial flow  $\mathbf{U}$ , together with the perturbations  $\tilde{\mathbf{u}}$ , take the form

$$\mathbf{u}(\mathbf{x}, t) = U(z)\hat{\mathbf{x}} + \tilde{\mathbf{u}}(z)e^{ik_x x + ik_y y - i\omega t}$$

In addition, there is a perturbation of the pressure field  $P(\mathbf{x})$ .

$$\delta P(\mathbf{x}) = \rho \tilde{P}(z)e^{ik_x x + ik_y y - i\omega t}$$

where we've again included a factor of  $\rho$  on the right-hand side to simplify subsequent equations.

This time we will perturb the full Navier-Stokes equation

$$\frac{\partial \mathbf{u}}{\partial t} + \mathbf{u} \cdot \nabla \mathbf{u} = -\frac{1}{\rho} \nabla P + \nu \nabla^2 \mathbf{u}$$

The linearised perturbation equations are

$$i(k_x U - \omega) \tilde{u}_x + \tilde{u}_z \frac{dU}{dz} = -ik_x \tilde{P} + \nu \left( \frac{d^2}{dz^2} - k_x^2 - k_y^2 \right) \tilde{u}_x \quad (5.59)$$

$$i(k_x U - \omega) \tilde{u}_y = -ik_y \tilde{P} + \nu \left( \frac{d^2}{dz^2} - k_x^2 - k_y^2 \right) \tilde{u}_y \quad (5.60)$$

$$i(k_x U - \omega) \tilde{u}_z = -\frac{d\tilde{P}}{dz} + \nu \left( \frac{d^2}{dz^2} - k_x^2 - k_y^2 \right) \tilde{u}_z \quad (5.61)$$

and the incompressibility condition is, as before,

$$ik_x \tilde{u}_x + ik_y \tilde{u}_y + \frac{d\tilde{u}_z}{dz} = 0 \quad (5.62)$$

We would like to derive a generalisation of the Rayleigh equation (5.47), now including the effects of viscosity. This is an equation just for  $\tilde{u}_z$ .

To achieve this, we first take the divergence of the Navier-Stokes equation which, after using the incompressibility condition  $\nabla \cdot \mathbf{u} = 0$ , gives

$$\frac{1}{\rho} \nabla^2 P = -2 \frac{dU}{dz} \frac{\partial u_z}{\partial x} \Rightarrow \left( \frac{d^2}{dz^2} - k_x^2 - k_y^2 \right) \tilde{P} = -2ik_x \frac{dU}{dz} \tilde{u}_z$$

If we now take  $\nabla^2$  of the third equation (5.61) (which really means multiplying by  $(d^2/dz^2 - k_x^2 - k_y^2)$ ), then we get a fourth order differential equation for  $\tilde{u}_z$ ,

$$\left[ i(k_x U - \omega) \left( \frac{d^2}{dz^2} - k_x^2 - k_y^2 \right) - ik_x \frac{d^2 U}{dz^2} - \nu \left( \frac{d^2}{dz^2} - k_x^2 - k_y^2 \right)^2 \right] \tilde{u}_z = 0 \quad (5.63)$$

This is the *Orr-Sommerfeld equation*. If we set  $k_y = 0$  then, in the limit  $\nu \rightarrow 0$  (which, as always, should really be thought of as the limit  $Re \rightarrow \infty$ ) it reduces to the Rayleigh equation (5.47).

We want to impose the no-penetration boundary condition  $\tilde{u}_z = 0$  and also the no-slip boundary condition  $\tilde{u}_x = \tilde{u}_y = 0$  at the edges of the flow. From (5.62), no-slip implies that  $\tilde{u}'_z = 0$ . But that still leaves the other linear combination of  $\tilde{u}_x$  and  $\tilde{u}_y$  which we recognise as the vorticity normal to the edge,

$$\zeta := \boldsymbol{\omega} \cdot \hat{\mathbf{z}} = ik_x \tilde{u}_y - ik_y \tilde{u}_x$$

We'll impose  $\zeta = 0$  at the boundary. But we can also look at the dynamics of this component of vorticity in the interior of the flow. By taking suitable linear combinations of (5.59) and (5.60) ( $k_y$  of the first minus  $k_x$  of the second) we get

$$\left[ i(k_x U - \omega) - \nu \left( \frac{d^2}{dz^2} - k_x^2 - k_y^2 \right) \right] \zeta = ik_y \frac{dU}{dz} \tilde{u}_z \quad (5.64)$$

This is the *Squire equation*. We should solve it in conjunction with the Orr-Sommerfeld equation (5.63), with the velocity perturbations  $\tilde{u}_z$  acting as a source for the vorticity perturbations  $\zeta$ .

In the limit  $\nu = 0$  we have no possibility of interesting vorticity fluctuations since  $\zeta$  is fully determined by the velocity perturbation  $\tilde{u}_z$ . However, the presence of viscosity turns the algebraic relation into a differential equation and this has more interesting solutions. In particular, we can have vorticity perturbations  $\zeta \neq 0$  even when  $\tilde{u}_z = 0$ . These are known as *Squire modes*.

**Claim:** Squire modes are always damped. This means that the vorticity doesn't lead to an instability unless driven by the velocity perturbation  $\tilde{u}_z$ .

**Proof:** The proof uses the same kind of trick that we saw when deriving the Rayleigh criterion. We multiply the homogeneous Squire equation by the complex conjugate  $\zeta^*$  and integrate over the width of the flow. After integrating by parts and imposing the boundary condition  $\zeta = 0$  at  $z = \pm h$ , we have

$$\nu \int_{-h}^{+h} dz \left( \left| \frac{d\zeta}{dz} \right|^2 + (k_x^2 + k_y^2) |\zeta|^2 \right) = - \int_{-h}^{+h} dz i(k_x U - \omega) |\zeta|^2$$

Taking the real part gives

$$\nu \int_{-h}^{+h} dz \left( \left| \frac{d\zeta}{dz} \right|^2 + (k_x^2 + k_y^2) |\zeta|^2 \right) = -\text{Im}(\omega) \int_{-h}^{+h} dz |\zeta|^2$$

Clearly the left-hand side is positive if  $\zeta \neq 0$ . So the right-hand side must also be positive which means that  $\text{Im}(\omega) < 0$ . But the fluctuations evolve as  $e^{-i\omega t} \sim e^{\text{Im}(\omega)t}$  so for  $\text{Im}(\omega) < 0$  these are decaying modes.  $\square$

### 5.5.1 Poiseuille Flow Revisited

To finish this section, we return to Poiseuille flow, restricted to a plane. Recall from Section 3.2 that Poiseuille flow is driven by a constant pressure gradient, with the background velocity field taking the parabolic form

$$U(z) = \alpha(h^2 - z^2)$$

for some constant  $\alpha$ . We define the Reynolds number for this flow to be

$$Re = \frac{U_{\max} h}{\nu} = \frac{\alpha h^3}{\nu}$$

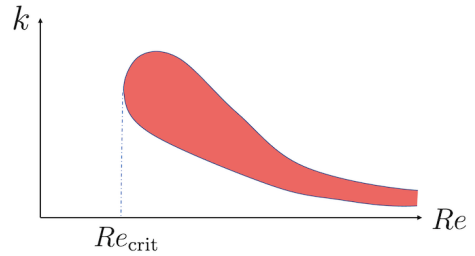
To determine the stability of Poiseuille flow, our task is clear. We look for perturbations with  $k_y = 0$  and  $k_x = k$  and try to solve the Orr-Sommerfeld equation

$$\left[ i(kU - \omega) \left( \frac{d^2}{dz^2} - k^2 \right) - ik \frac{d^2 U}{dz^2} - \nu \left( \frac{d^2}{dz^2} - k^2 \right)^2 \right] \tilde{u}_z = 0$$

We view this as an eigenvalue equation, with both the eigenfunction  $\tilde{u}_z$  and the eigenvalue  $\omega$  to be determined. The flow is unstable if there exists solutions with  $\text{Im}(\omega) > 0$ .

This is not a computation that can be done analytically and the equation must be solved numerically<sup>14</sup>. One finds that there is no instability for low Reynolds number, but Poiseuille flow becomes unstable for any Reynolds number beyond the critical value

$$Re > Re_{\text{crit}} \approx 5772$$



The range of unstable  $k$ -values for a given Reynolds number takes the form of the red region shown in the figure.

There's something rather surprising about this result. By now we're used to viscosity acting as a dampening force, causing perturbations to die away. But here it plays the opposite role! Without viscosity, Poiseuille flow is linearly stable. Viscosity causes it to become unstable at high Reynolds number.

<sup>14</sup>This was done by Orszag in 1971 in [this paper](#) where the critical Reynolds number was first calculated.

This is far from the last word on instabilities. The linear analysis sketched above suggests that Couette flow should be stable for all  $Re$  while Poiseuille flow should break down only for  $Re \approx 6000$ . Neither of these agrees well with experiment. Instead, Couette flow is turbulent by  $Re \approx 400$  while Poiseuille flow is typically turbulent by  $Re \approx 2000$ . This shows up the failure of our simple linear analysis. While the flows are stable against infinitesimally small perturbations, fluctuations whose amplitude grows beyond some critical value can push them over the edge. The instability is akin to a first order phase transition in thermodynamics, or to a tunnelling event in quantum mechanics, with some finite barrier to cross.